doi:10.1093/jmcb/mjz002
Published online March 18, 2019

Article

Morphine induces dysfunction of PINK1/Parkin-mediated mitophagy in spinal cord neurons implying involvement in antinociceptive tolerance

Hong Kong[1,†], Chun-Yi Jiang[1,†,*], Liang Hu[1,†], Peng Teng[1], Yan Zhang[1,2], Xiu-Xiu Pan[1], Xiao-Di Sun[1,3], and Wen-Tao Liu[1,4,*]

[1] Neuroprotective Drug Discovery Key Laboratory of Nanjing Medical University, Department of Pharmacology, Nanjing Medical University, Nanjing, China
[2] Research Division of Pharmacology, China Pharmaceutical University, Nanjing, China
[3] Department of Anesthesiology, The First Affiliated Hospital of Nanjing Medical University, Nanjing, China
[4] Department of Pharmacy, Sir Run Run Shaw Hospital Affiliated to Nanjing Medical University, Nanjing, China
[†] These authors contributed equally to this work.
* Correspondence to: Chun-Yi Jiang, E-mail: jcy@njmu.edu.cn; Wen-Tao Liu, E-mail: painresearch@njmu.edu.cn

Edited by Xuebiao Yao

The development of opioid-induced analgesic tolerance is a clinical challenge in long-term use for managing chronic pain. The mechanisms of morphine tolerance are poorly understood. Mitochondria-derived reactive oxygen species (ROS) is a crucial signal inducing analgesic tolerance and pain. Chronic administration of morphine leads to robust ROS production and accumulation of damaged mitochondria, which are immediately removed by mitophagy. Here, we show that morphine inhibits mitochondria damage-induced accumulation of PTEN-induced putative kinase 1 (PINK1) in neurons. It interrupts the recruitment of Parkin to the impaired mitochondria and inhibits the ubiquitination of mitochondrial proteins catalyzed by Parkin. Consequently, morphine suppresses the recognition of autophagosomes to the damaged mitochondria mediated by LC3 and sequestosome-1 (SQSTM1/p62). Thus, morphine inhibits autophagy flux and leads to the accumulation of SQSTM1/p62. Finally, the impaired mitochondria cannot be delivered to lysosomes for degradation and ultimately induces robust ROS production and morphine tolerance. Our findings suggest that the dysfunction of mitophagy is involved in morphine tolerance. The deficiency of PINK1/Parkin-mediated clearance of damaged mitochondria is crucial for the generation of excessive ROS and important to the development of analgesic tolerance. These findings suggest that the compounds capable of stabilizing PINK1 or restoring mitophagy may be utilized to prevent or reduce opioid tolerance during chronic pain management.

Keywords: mitophagy, PINK1, Parkin, ROS, SQSTM1/p62, morphine tolerance

Introduction

Chronic pain as a serious public health problem afflicts millions of people in the world (Renfrey et al., 2003). Opioids, such as morphine, play an important role in pain relief. Although lots of opioids were discovered, morphine remains the most effective drug for the treatment of severe pain. However, long-term use of morphine leads to analgesic tolerance and hyperalgesia, which greatly reduce the utilization of this drug (Bekhit, 2010; Morgan and Christie, 2011). For several decades, numerous studies have been devoted to understanding the mechanisms underlying morphine tolerance. Great progress was made and the investigations mainly focused on the neuronal actions and non-neuronal actions. With regard to neuronal actions, morphine can cause β-arrestin-dependent internalization and protein kinase C (PKC)-associated desensitization of μ-opioid receptor (MOR) (Macey et al., 2006; Bailey et al., 2009; Miyatake et al., 2009). Furthermore, morphine could block long-term potentiation of inhibitory synapses and brief treatment with morphine blocked LTP_{GABA} (Nugent et al., 2007). In addition, many investigations suggested that long-term use of morphine upregulated the phosphorylation of N-methyl-D-aspartic acid (NMDA) receptor (Martin et al., 1999; Hutchinson et al., 2011). The activated NMDA receptor exhibited enhanced calcium conductance in neurons. As a result, these potentiated neuronal excitabilities finally developed tolerance (Viviani et al., 2003; Kleibeuker et al., 2007).

Received March 1, 2018. Revised July 1, 2018. Accepted January 28, 2019.

In contrast, with regard to non-neuronal actions of morphine, it was proved that morphine could induce central immune responses. In addition to binding with MOR, morphine as an exogenous ligand could be recognized by Toll-like receptor 4 (TLR4) accessory protein, myeloid differentiation protein 2 (MD-2), inducing neuroinflammation (Wang et al., 2012). Blockade of TLR4/MD2 suppresses morphine tolerance (Hutchinson et al., 2012). Furthermore, long-term administration of morphine activated NLRP3 inflammasome in spinal cord and then caused tolerance (Cai et al., 2016). Morphine-induced reactive oxygen species (ROS) derived from mitochondria is a crucial factor for the activation of NLRP3 inflammasome and ROS scavenger could significantly suppress morphine tolerance (Cai et al., 2016).

ROS is a side product during oxidative phosphorylation and the major source of intracellular ROS comes from mitochondria (Balaban et al., 2005; Wallace et al., 2010). ROS acts as a positive regulator of adenosine 5′-monophosphate (AMP)-activated protein kinase (AMPK), which is activated by a low ATP/AMP ratio upon mitochondrial dysfunction (Zong et al., 2002; Dong et al., 2014) and contributes to the attenuation of neuropathic pain (Lu et al., 2017). Under pathological conditions, ROS increases and causes cell damage by impairing organelles and leading to mutations of genome (Tait and Green, 2010). Therefore, the accumulated ROS from mitochondria should be detoxified and the damaged mitochondria must be cleared. ROS could induce the translocation of Parkin to the damaged mitochondria, initiating mitophagy to clear damaged mitochondria (Narendra et al., 2008). Mitophagy is an evolutionarily conserved cellular process. It is a fundamental process critical for maintaining mitochondrial fitness, especially, for mitochondrial quality control. Mitophagy is induced by the loss of mitochondrial membrane potential (MMP) or the accumulation of misfolded proteins. During mitophagy, PINK1 is stabilized on the outer mitochondrial membrane (OMM) instead of being imported into mitochondria (Narendra et al., 2010), and PINK1 activates Parkin ubiquitin ligase by phosphorylating Parkin and ubiquitin (Kane et al., 2014; Kazlauskaite et al., 2014; Eiyama and Okamoto, 2015). After activation and recruitment to mitochondria, Parkin mediates the engulfment of mitochondria by autophagosomes and the selective elimination of impaired mitochondria (Narendra et al., 2008). In the previous study, we found that morphine increased MDA level in the spinal cord (Cai et al., 2016). It implicated that the chronic administration of morphine could induce excessive ROS; however, the mechanism was poorly understood. Here, we unravel the key steps of morphine to interrupt PINK1/Parkin-mediated mitophagy, thereby probably providing a link between mitophagy dysfunction and morphine tolerance.

Results

Chronic administration of morphine induces excessive generation of ROS and accumulation of damaged mitochondria

Variety of stress markedly induces mitochondrial ROS production (Brookes et al., 2004). It was reported that the accumulative ROS was associated with morphine tolerance and addiction (Kim et al., 2004; Ma et al., 2015; Cai et al., 2016). To study the effects of morphine on ROS and mitochondria, the animal model for morphine tolerance was utilized. Daily intrathecal injection of 10 μg/10 μl morphine for 7 days led to a time-dependent decrease in morphine's maximal possible effect (MPE). MPE on Days 3, 5, and 7 was reduced to 44.5% ($P < 0.001$), 31.4% ($P < 0.001$), and 19.3% ($P < 0.001$), respectively (Figure 1A). Based on behavioral test, we next examined the level of ROS in the spinal cord. Chronic administration of morphine induced significant increase in ROS level (Figure 1B and C). Mitochondria are the main source of cellular ROS. It was reported that the deficiency of quality control mechanism, mitophagy, led to accumulation of damaged mitochondria and excessive ROS (Eiyama and Okamoto, 2015). In order to investigate whether morphine led to the impairment of mitochondria or not, phosphorylation level of AMPK was examined as an indicator for mitochondria quality. Our results showed that morphine increased the phosphorylation of AMPK α subunit (Thr172) (Figure 1D), suggesting that morphine caused mitochondria damage. Furthermore, we investigated the levels of Bax and Bcl-2. Bax was reported to translocate from cytosol to mitochondria inducing permeabilization of the OMM (Martinou and Green, 2001). In contrast with Bax, Bcl-2 could interact with Bax inhibiting the mitochondrial permeability transition and cytochrome c release (Kluck et al., 1997; Yang et al., 1997). Immunoblots showed that the acute administration of morphine led to an increase in the ratio of Bax/Bcl-2 at 24 hand the chronic administration of morphine increased the ratio of Bax/Bcl-2 from Day 1 to Day 7 (Figure 1F and G), suggesting that morphine induced mitochondria damage. Furthermore, electron microscopy (EM) was utilized to assess mitochondrial integrity and state. Results showed that morphine induced the accumulation of swollen mitochondria in the spinal cord and caused mitochondria damage (Figure 1E).

Morphine activates the initiation of autophagy and leads to the accumulation of SQSTM1/p62 protein

Morphine induced accumulation of damaged mitochondria. The damaged mitochondria would evoke mitophagy, a quality control process that sequesters and digests impaired mitochondria (Ding and Yin, 2012). This process is stimulated through the coordinated activation of several multiprotein complexes, such as ULK1/2, Beclin 1, Atg 5, and LC3. Finally, the damaged mitochondria are targeted by autophagosomes mediated by the autophagic adaptor SQSTM1/p62 (Bjorkoy et al., 2005; Pankiv et al., 2007; Kim et al., 2008). Therefore, we investigated the effects of morphine on this process. The protein levels of autophagy-related markers, including Beclin 1, Atg 5, LC3, and SQSTM1/p62, were assessed by western blotting. Immunoblots showed that morphine upregulated Atg 5 level after 24 h of administration and also increased Atg 5 level from Day 1 to Day 7. However, morphine did not affect the level of Beclin 1 (Figure 2A and B). Furthermore, Figure 2C showed that morphine increased the level of LC3-II by 31.3% after 24 h and LC3-II protein level on Day 7. However, the level of SQSTM1/p62 was not affected after 24 h of morphine administration but increased

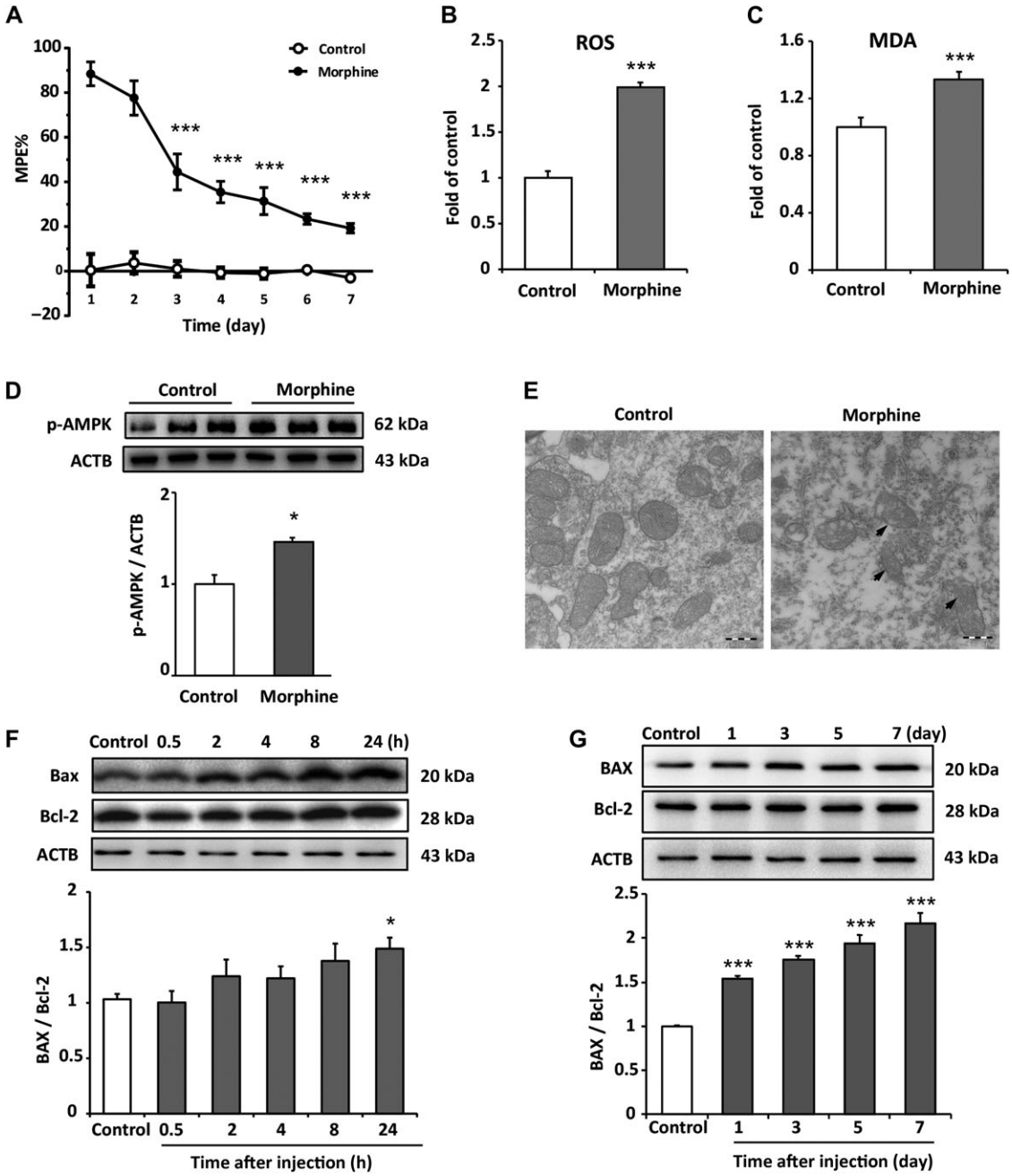

Figure 1 Chronic intrathecal administration of morphine induces excessive generation of ROS and causes accumulation of damaged mitochondria in spinal cord. (**A**) Tail-flick method was performed to evaluate morphine tolerance. Data are shown as percentage of MPE. Chronic administration reduced morphine's MPE from Day 3 to Day 7. The saline-treated group served as control. The MPE from Day 3 to Day 7 were 44.5%, 35.5%, 31.4%, 23.4%, and 19.3%, respectively. One-way ANOVA followed by Tukey's multiple comparisons test. $n = 8$, $^{***}P < 0.001$ vs. MPE of Day 1. (**B** and **C**) The levels of ROS and MDA on Day 7 from spinal cord tissue were assessed by DCFH-DA staining and MDA detection kit. The ROS level and MDA level increased by 99.1% and 32.9%, respectively, compared with control group. Student's *t*-test. $n = 6$, $^{***}P < 0.001$ vs. control group. (**D**) Increased phosphorylation of AMPK (Thr172) was detected in morphine-treated group compared with control group. Student's *t*-test. $n = 4$, $^{*}P < 0.05$ vs. control group. (**E**) Sections of spinal cord from mice chronically administrated with morphine were fixed and subjected to EM examination. Morphine induced a significant damage and accumulation of abnormal mitochondria compared with control group. Scale bar, 500 nm. (**F** and **G**) Morphine increased the ratio of Bax/Bcl-2 after 24 h of administration; in long-term treatment, morphine significantly increased the ratio of Bax/Bcl-2 from Day 1 to Day 7. $n = 4$, $^{*}P < 0.05$, $^{***}P < 0.001$ vs. control group.

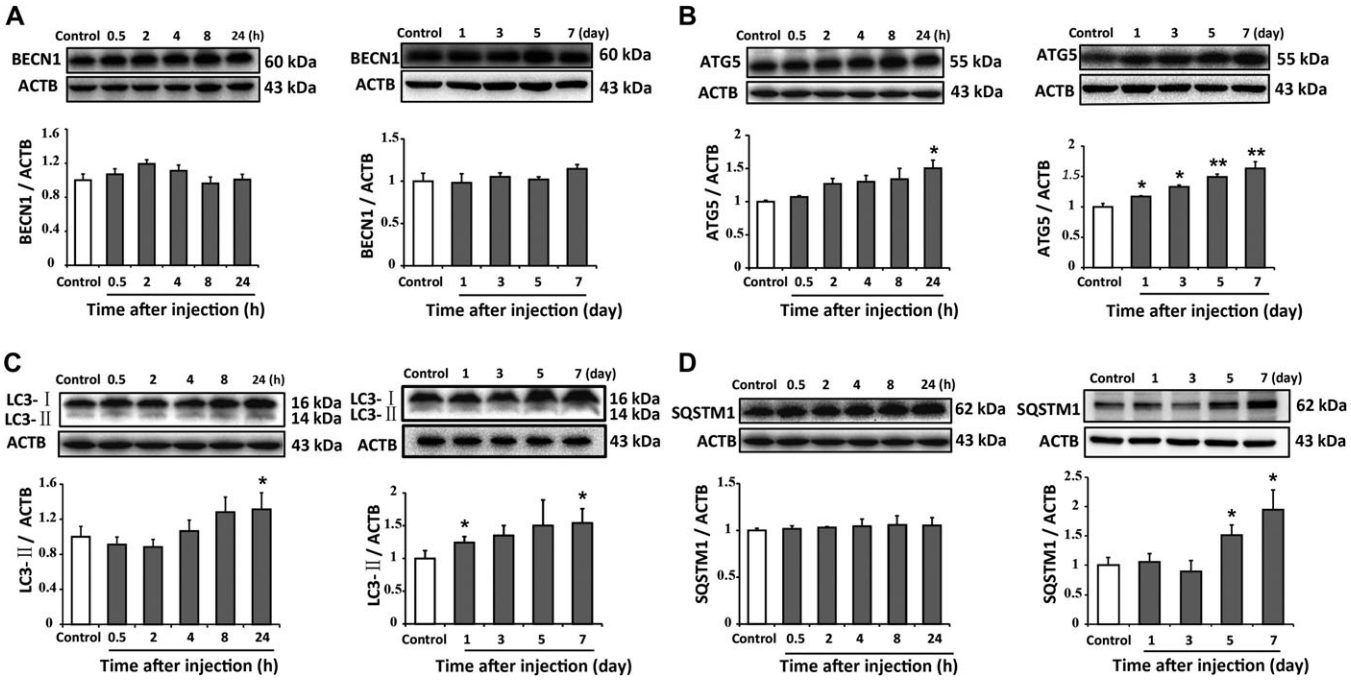

Figure 2 Morphine activates the initiation of autophagy and leads to the accumulation of SQSTM1/p62 protein. Repeated intrathecal morphine injections affected the protein levels of BECN1, Atg 5, LC3-II, and SQSTM1 in the spinal cord of mice. Representative western blots and densitometric analysis summary (normalized to ACTB/actin loading control) are shown. (**A**) Morphine did not change the level of BECN1 after 7 days of intrathecal injection. (**B** and **C**) Morphine increased the levels of Atg 5 and LC3-II after 1 day of intrathecal injection. (**D**) Morphine increased the level of SQSTM1/p62 after 5 days of intrathecal injection. $n = 4$, $^{*}P < 0.05$, $^{**}P < 0.01$ vs. control group.

after seven consecutive days of administration (Figure 2D). We also utilized immunostaining to assess the effect of morphine on SQSTM1/p62 in the spinal cord. As shown in Figure 3A–C, morphine sufficiently elevated the number of reactive staining and increased the intensity of fluorescence staining for SQSTM1/p62 in neurons. Our data showed that chronic morphine administration activated the initiation of autophagy and led to the accumulation of SQSTM1/p62 protein in neurons of spinal cord dorsal horn.

Morphine induces the dysfunction of mitochondria and inhibits autophagic flux

Next, we investigated the effects of morphine on mitochondria in neurons with SH-SY5Y cells. JC-1 staining showed that morphine sufficiently decreased $\Delta\Psi_m$ (Figure 4A), while MitoSOX staining showed that morphine increased the level of ROS (Figure 4B). Our data indicated that morphine induced mitochondrial depolarization and dysfunction. To avoid cellular damage, ROS-generating and damaged mitochondria were removed by mitophagy (Goldman et al., 2010). As shown in Figure 4C, morphine increased the level of the autophagy marker LC3-II. In accordance with the *in vivo* study, morphine also increased the protein level of SQSTM1/p62 but not affected the mRNA level of SQSTM1/p62 (Supplementary Figure S1). Furthermore, naloxone suppressed morphine-inudced increase of LC3-II and SQSTM1/p62 (Figure 4C), suggesting the effect of morphine is the opioid receptor dependent.

Next, we assessed the levels of LC3-II and SQSTM1/p62 in the presence or absence of the inhibitor of lysosomal degradation in SH-SY5Y cells. Bafilomycin A1 was used in this study as an inhibitor of fusion between autophagosomes and lysosomes and as an inhibitor of lysosomal degradation. Western blot analysis showed that the level of LC3-II increased after the administration of rapamycin, morphine and bafilomycin A1 respectively comparing to control group (Figure 4D). In addition, morphine and bafilomycin A1 further increased the level of LC3-II induced by rapamycin. We also found that the increasing of LC3-II induced by bafilomycin A1 was higher than that induced by morphine (Figure 4D), it suggested that morphine did not generally inhibit the maturation of autophagosome like bafilomycin A1, but may specially disturb the delivery of damaged mitochondria to lysosomes. Furthermore, the level of SQSTM1/p62 was also increased in morphine and bafilomycin A1 groups comparing to control group. In addition, comparing with rapamycin group, morphine and bafilomycin A1 further increased the level of SQSTM1/p62 in the presence of rapamycin. These implied that the morphine enhanced the initiation of autophagy, however, inhibited autophagic flux. The autophagic flux was further monitored with the Tf-LC3 Assay (Law et al., 2014), which relies on the different nature of GFP and RFP fluorescence under acidic conditions. GFP fluorescence is sensitive to the acidic condition of the lysosome lumen, while RFP is relatively stable under acidic conditions. Therefore, the colocalization of GFP and RFP fluorescence (yellow puncta) indicates the phagophores or autophagosomes that have not fused with lysosomes, whereas

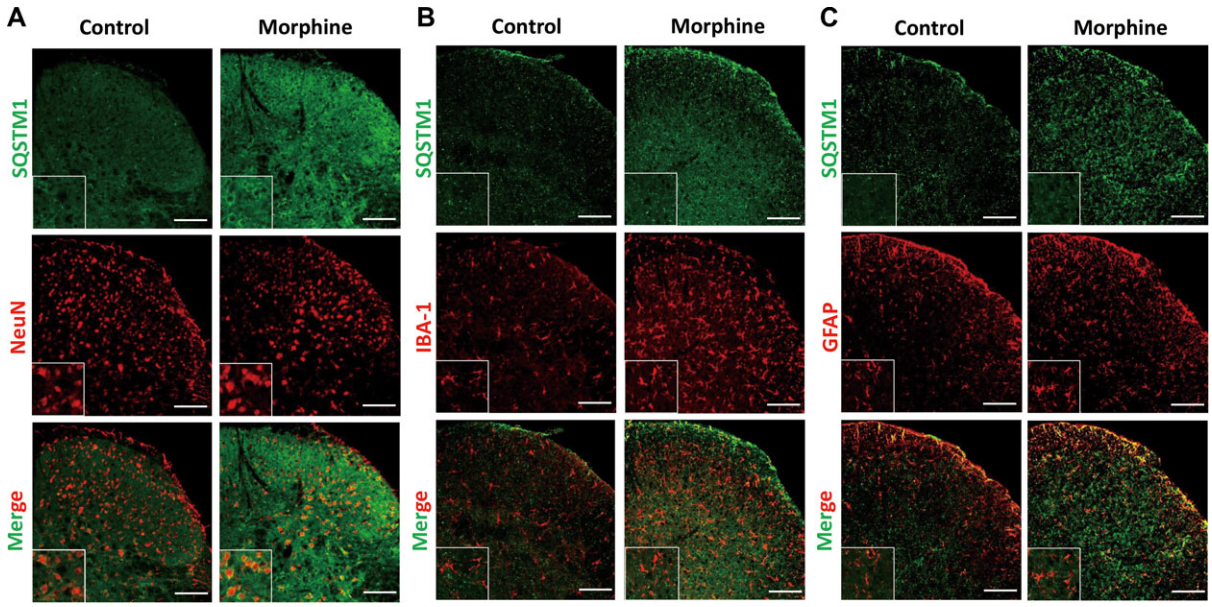

Figure 3 The distribution and cellular location of SQSTM1/p62 after seven consecutive days of morphine intrathecal injection in the spinal cord dorsal horn. Sections of spinal cord from mice chronically administrated with morphine were fixed and subjected to double immunofluorescence stain. Confocal microscopy was performed to determine the co-localization of SQSTM1/p62 (green) and neuron (NeuN, red), microglia (IBA-1, red), or astrocyte (GFAP, red). Spinal samples were collected after the last administration of morphine. NeuN, neuronal nuclear protein; IBA-1, ionized calcium-binding adapter molecule 1; GFAP, glial fibrillary acidic protein. Scale bar, 100 μm.

RFP-only fluorescence (red puncta) indicates the autolysosomes. In our study, Hank's buffered salt solution (HBSS) and rapamycin were used to induce autophagic flux (Keil et al., 2013). The confocal microscopic scanning demonstrated that HBSS and rapamycin treatment increased red puncta in cells (Figure 4E), while in the presence of morphine, yellow puncta were increased in cells (Figure 4E). It indicated that morphine inhibited the autophagic flux.

Morphine inhibits mitophagy by suppressing recruitment of Parkin to the damaged mitochondria and decreasing the ubiquitination of mitochondrial proteins

Morphine induces accumulation of damaged mitochondria and inhibits autophagic flux. We firstly investigated the effect of morphine on lysosomes. The LysoSensor Green, a lysosomal pH indicator, was utilized to investigate the acidity of lysosomes. Flow cytometry and confocal microscope analysis indicated that morphine did not affect lysosomal pH. Furthermore, we also measured the level of lysosomal associated membrane protein 1 (LAMP1), which was involved in lysosomal exocytosis, lysosomal movement, and the fusion of phagosomes with lysosomes. However, we did not find that morphine affected the level of LAMP1 (Supplementary Figure S2). Therefore, we considered that whether morphine suppressed mitophagy by interrupting the recognition of autophagosomes to the damaged mitochondria. Firstly, we investigated the effect of morphine to mitophagy. CCCP was utilized to induced mitophagy in SH-SY5Y cells (Geisler et al., 2010). Immunoblots showed that CCCP led to the degradation of mitochondrial protein Tom20 and COX IV indicating that the damaged mitochondria were cleaned by mitophagy. However, morphine inhibited the decreasing of Tom20 and COX IV induced by CCCP. It suggested that morphine interrupted the process of mitophagy (Figure 5A). To further confirm the effect of morphine on mitophagy, we investigated the recruitment of Parkin to the impaired mitochondria induced by CCCP. Parkin, an ubiquitin ligase, is recruited to the mitochondria depending on decline of $\Delta\Psi_m$ and it is dependent on the accumulation of PINK1 on the surface of mitochondria with low $\Delta\Psi_m$, leading to the ubiquitination outer membrane proteins (Chen et al., 2010; Geisler et al., 2010; Youle and Narendra, 2011). Then, the autophagic adaptor protein SQSTM1/p62 is recruited to the clustered mitochondria and is degraded together with damaged mitochondria. SH-SY5Y cells were administrated with CCCP in or not in presence of morphine, and then subcellular fractionation of mitochondria was collected for further study. Immunoblots showed that CCCP significantly increased the level of Parkin in mitochondria, however, morphine inhibited the recruitment of Parkin to mitochondria caused by CCCP (Figure 5B). To verify the Parkin recruitment to the mitochondria observed by western blotting, we further performed confocal microscopic scan. The data showed that CCCP obviously induced the recruitment of Parkin to the mitochondria; however, morphine inhibited the recruitment of Parkin (Figure 5E). It was reported that PINK1-mediated phosphorylation of Parkin S65 was important for the activation and mitochondrial localization of Parkin (Kondapalli

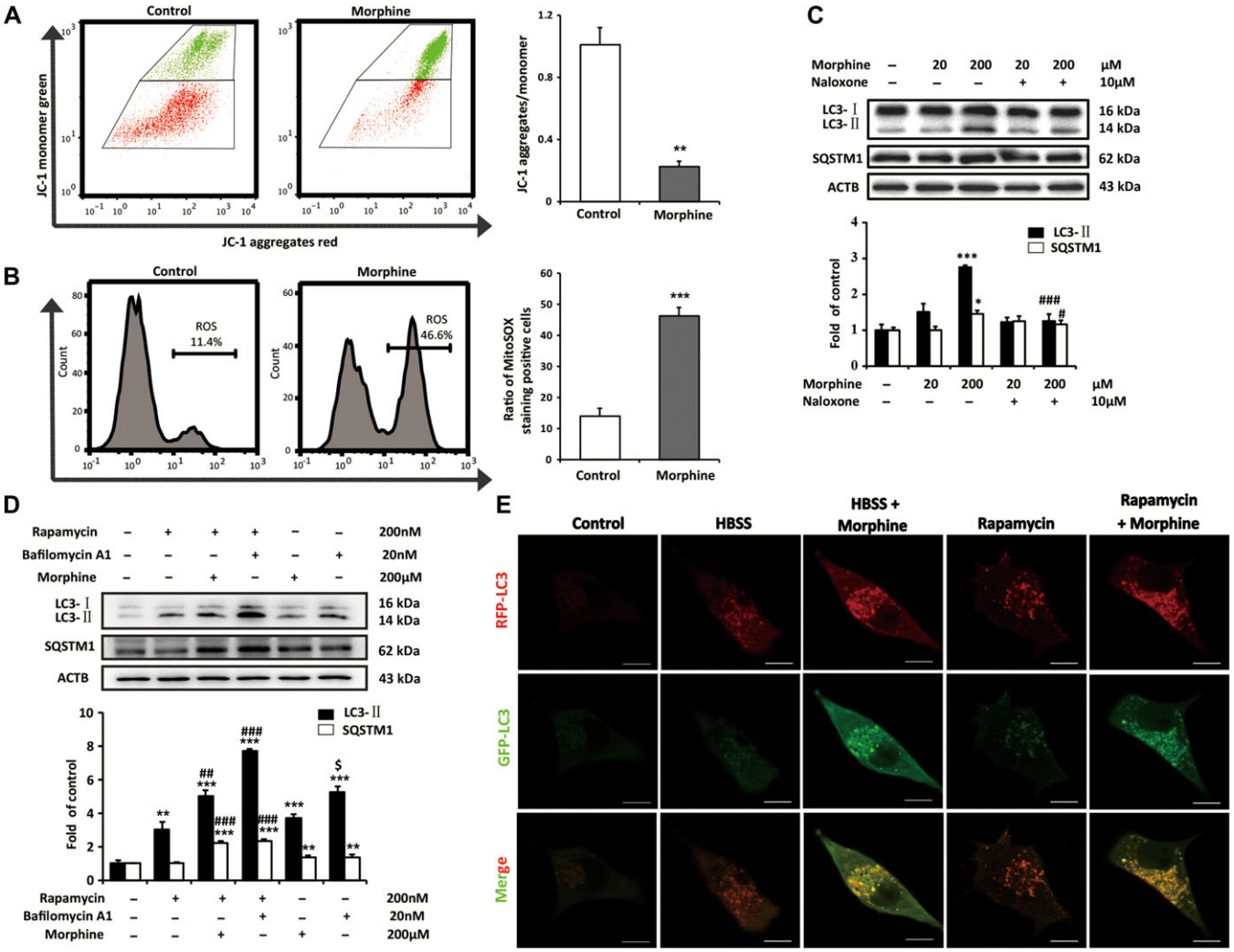

Figure 4 Morphine induces mitochondria damage and increases ROS in neuron by the inhibition of autophagic flux. (**A** and **B**) SH-SY5Y cells were stimulated with morphine (200 μM) for 24 h. The effects of morphine on $\Delta\Psi_m$ were determined by calculating the percentage of JC-1 aggregates/monomer in 10000 cells. The level of ROS was assessed by calculating the percentage of MitoSOX staining-positive cells in 10000 cells. Student's *t*-test. $n = 3$, $^{**}P < 0.01$, $^{***}P < 0.001$ vs. control group. (**C**) SH-SY5Y cells were treated with morphine (20 or 200 μM) with or without of naloxone (10 μM) for 24 h. One-way ANOVA followed by Tukey's multiple comparisons test. $n = 3$, $^{*}P < 0.05$, $^{***}P < 0.001$ vs. control group, $^{\#}P < 0.05$, $^{\#\#\#}P < 0.001$ vs. morphine (200 μM) group. (**D**) SH-SY5Y cells were treated with or without rapamycin (200 nM) or Bafilomycin A1 (20 nM) in the presence or absence of morphine (200 μM) for 24 h. One-way ANOVA followed by Tukey's multiple comparisons test. $n = 3$, $^{**}P < 0.01$, $^{***}P < 0.001$ vs. control group, $^{\#\#}P < 0.01$, $^{\#\#\#}P < 0.001$ vs. rapamycin group, $^{\$}P < 0.05$ vs. morphine group. (**E**) SH-SY5Y cells were transfected with the tandem fluorescent mRFP-GFP-LC3 adenoviral vector, and then treated with HBSS for 2.5 h, rapamycin (200 nM) for 24 h, and morphine (200 nM) for 24 h. Scale bar, 10 μm.

et al., 2012). Therefore, we assessed the phosphorylation of Parkin S65 and the ubiquitination of mitochondrial proteins upon the treatment of CCCP or/and morphine. We utilized lysate of SH-SY5Y cells to access the phosphorylation of Parkin S65. Immunoblots showed that CCCP increased phosphorylation of Parkin S65; however, morphine inhibited the phosphorylation of Parkin S65 induced by CCCP (Figure 5C). We utilized mitochondria fractionation to access the ubiquitination, the results showed that CCCP increased the level of ubiquitination, however, morphine inhibited the upregulation of ubiquitination caused by CCCP (Figure 5D).

Morphine interrupts the recognition of autophagosomes to the damaged mitochondria and inhibits the infusion of damaged mitochondria to lysosomes

It was reported that during mitophagy the damaged mitochondria recruited the autophagic adaptor SQSTM1/p62 to mitochondrial clusters. As an autophagy-specific substrate, SQSTM1/p62 interacts with LC3-II mediating the recognition of autophagosomes to the damaged mitochondria. Finally, the damaged mitochondria were delivered to lysosomes mediated by autophagosomes. We wanted to investigate whether morphine could affect the recognition of autophagosomes to the

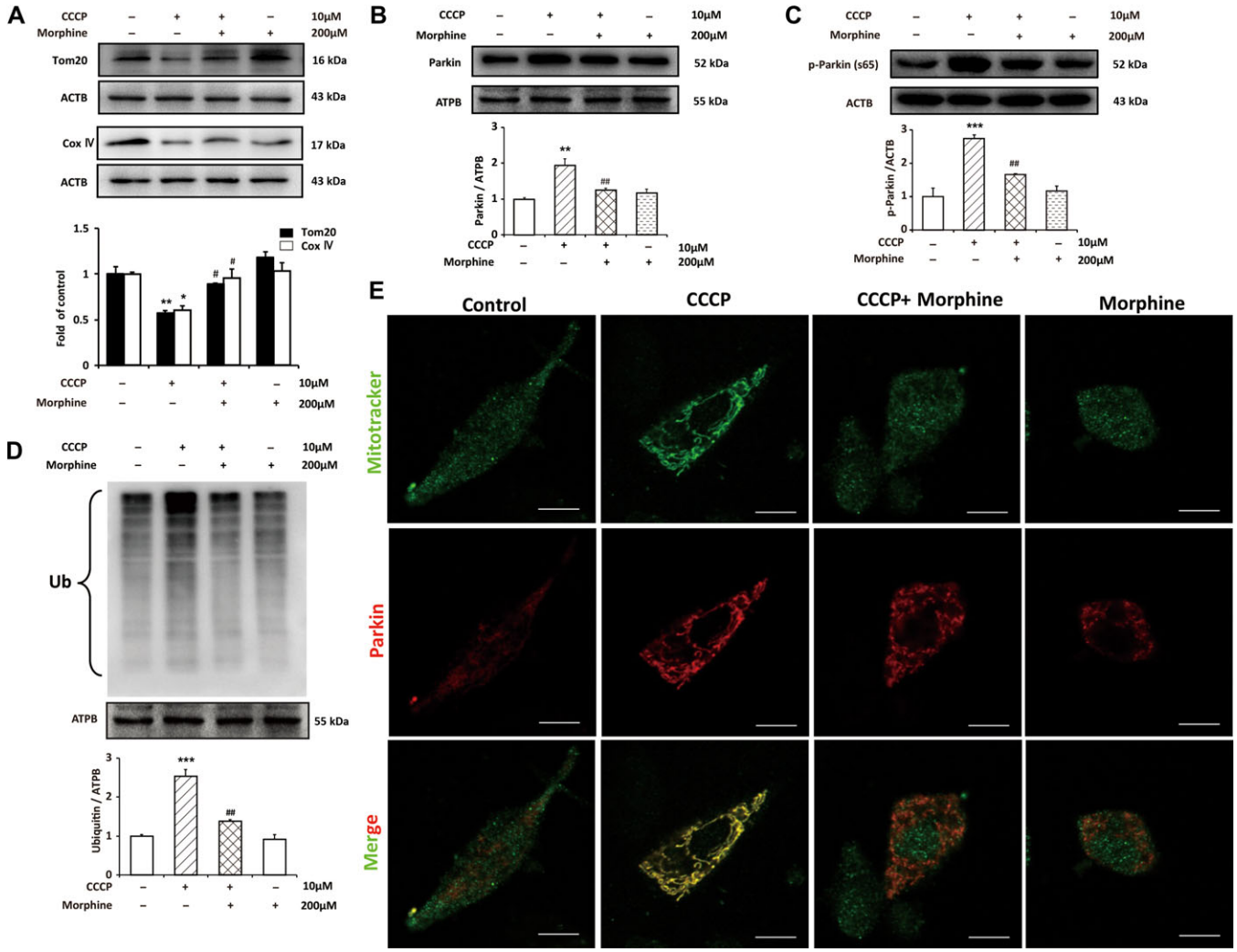

Figure 5 Morphine inhibits mitophagy by suppressing recruitment of Parkin to the damaged mitochondria and decreasing the ubiquitination of mitochondrial proteins. SH-SY5Y cells were treated with CCCP (10 μM) for 2.5 h with or without morphine (200 μM) for 24 h. (**A** and **C**) The levels of Tom20, COX IV, and the phosphorylation of Parkin (Ser65) from whole-cell extract were analyzed by western blotting. (**B** and **D**) The levels of Parkin and ubiquitylated proteins in mitochondria were analyzed by western blotting. $n = 3$, $^{*}P < 0.05$, $^{**}P < 0.01$, $^{***}P < 0.001$ vs. control group, $^{\#}P < 0.05$, $^{\#\#}P < 0.01$ vs. CCCP group. (**E**) SH-SY5Y cells were treated with CCCP (10 μM) for 2.5 h with or without morphine (200 μM) for 24 h, and then labeled with Mitotracker green and stained with anti-Parkin antibody (red). Scale bar, 10 μm.

damaged mitochondria and the delivery of impaired mitochondria to lysosomes. Rotenone, the mitochondrial complex I inhibitor was utilized to induced mitochondria damage (Zhou et al., 2011). The confocal microscopic scanning showed that autophagy-associated LC3-RFP puncta accumulated around mitochondria after the treatment of rotenone (Figure 6A). We investigated the effects of morphine to the recognition between LC3 and mitochondria. Our study indicated that in the presence of morphine, rotenone induced LC3-RFP puncta did not colocalize with damaged mitochondria (Figure 6A). Furthermore, our data manifested that morphine also induced the formation of LC3-RFP puncta and the puncta did not colocalize with mitochondria (Figure 6A). These indicated that morphine interrupted the recognition of autophagosomes to the damaged mitochondria. In addition, we respectively labeled mitochondria and lysosomes with mitotracker green and lysotracker red. The confocal microscopic scanning demonstrated that morphine interrupted infusion of damaged mitochondria and lysosomes (Figure 6B). Furthermore, we used LC3-GFP and lysotracker red respectively labeled autophagosomes and lysosomes. The data showed that rotenone induced the infusion of autophagosomes to lysosomes (Figure 6C); however, morphine inhibited the infusion caused by rotenone. Furthermore, morphine also activated lysosomes without rotenone, and inhibited the infusion of autophagosomes to lysosomes (Figure 6C). According to the results above, morphine interrupted the recognition of autophagosomes to the damaged mitochondria and inhibited the infusion of damaged mitochondria to lysosomes.

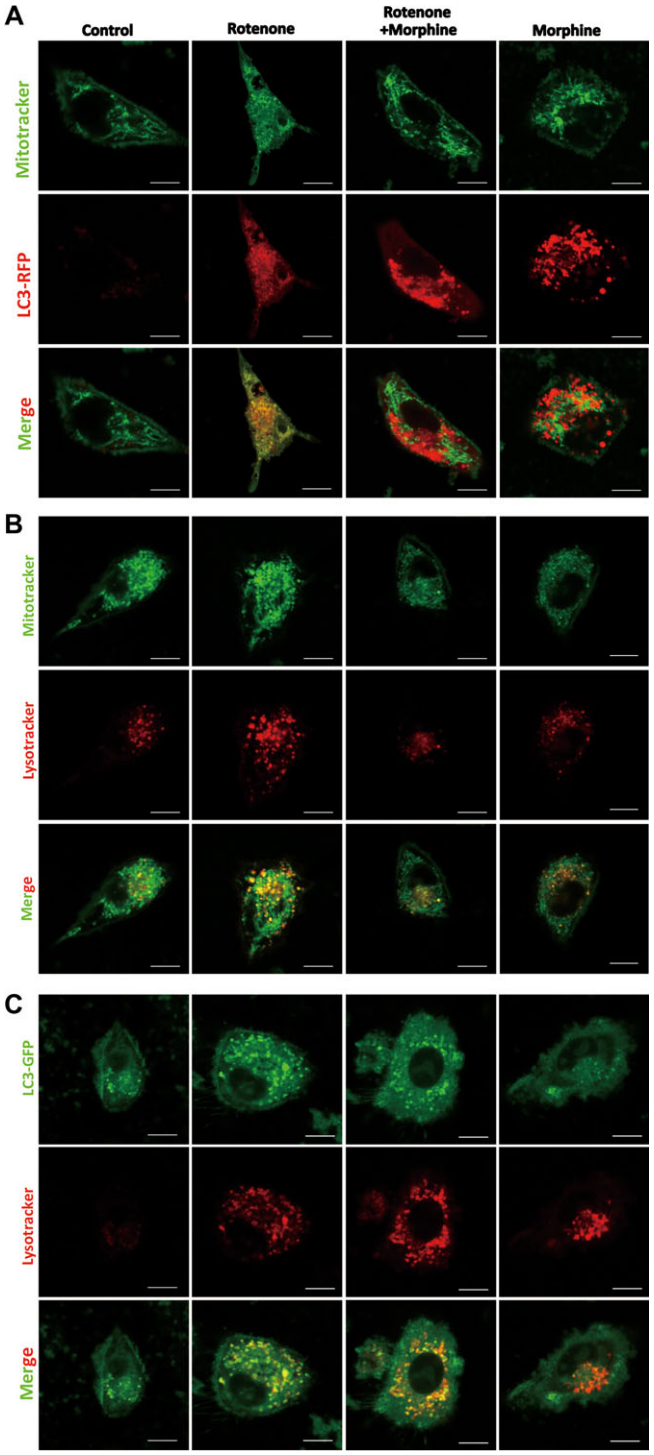

Figure 6 Morphine interrupts the recognition of autophagosomes to the damaged mitochondria and suppresses the infusion of damaged mitochondria to lysosomes. (**A**) SH-SY5Y cells expressing RFP-LC3 were stimulated with rotenone (100 nM) for 6 h, in the presence or absence of morphine (200 μM) for 24 h, and then stained with Mitotracker green for mitochondria. (**B**) SH-SY5Y cells were stimulated with rotenone (100 nM) for 6 h, in the presence or absence of morphine (200 μM) for 24 h, and then stained with Mitotracker green for mitochondria and Lysotracker red for lysosomes. (**C**) SH-SY5Y cells expressing GFP-LC3 were stimulated with rotenone (100 nM) for 6 h, in the presence or absence of morphine (200 μM) for 24 h, and then stained with Lysotracker red for lysosomes. Scale bar, 10 μm.

Morphine induces the degradation of PINK1 under stress and the rescue of PINK1 improves mitophagy deficiency caused by morphine

PINK1 and Parkin sense and mark the dysfunctional mitochondria in mammalian cells. In this process, PINK1 plays an important role. It is a prerequisite for Parkin activation and translocation. Therefore, we wanted to examine whether the PINK1 was affected by morphine. In normal condition, PINK1 is usually kept at an undetectable level in cells (Greene et al., 2012). When mitochondria lose membrane potential, PINK1 accumulates but not be degraded by protease (Youle and Narendra, 2011). CCCP was utilized to induce the loss of $\Delta\Psi_m$. Immunoblots showed that CCCP sufficiently increased the level of PINK1 in SH-SY5Y cells, however, morphine inhibited the CCCP-induced accumulation of PINK1 (Figure 7A). It implied that morphine induced the degradation of PINK1. It was mentioned above that morphine led to the accumulation of SQSTM1/p62, and also inhibited the autophagic flux. Therefore, we sought to examine whether PINK1 overexpression could improve morphine-induced dysfunction of mitophagy. We utilized lentivirus-mediated PINK1 overexpression, and the immunoblots showed that the rescue of PINK1 decreased the accumulation of SQSTM1/p62 caused by morphine (Figure 7B and C). Our study suggested that, in the presence of morphine, PINK1 was not stable on damaged mitochondria, even with declined $\Delta\Psi_m$. As a result, the damaged mitochondria could not be removed, and autophagic substrate accumulated.

Discussion

Recently, the identified pathways that mediate mitophagy in mammalian cells include NIP3-like protein X (NIX)-mediated mitophagy in red blood cells (Schweers et al., 2007) and PINK1–Parkin-mediated mitophagy in most mammalian cells. PINK1 and Parkin act cooperatively in detecting the state of mitochondria and marking damaged mitochondria for disposal via mitophagy. When mitochondria lose membrane potential, PINK1 is stabilized on the OMM and activates parkin ubiquitin ligase activity. Autophagy receptors, such as SQSTM1/p62, bind to ubiquitinated cargo and LC3-coated phagophores to mediate mitophagy. In this study, we found that the administration of morphine promoted the degradation of PINK1 even the mitochondria were impaired. As a result, Parkin was not recruited to the mitochondria with low $\Delta\Psi_m$, the mitochondrial proteins could not be ubiquitylated, and the damaged mitochondria could not be recognized by autophagosomes. Therefore, morphine interrupted the recognition of autophagosomes to the damaged mitochondria and inhibited the delivery of impaired mitochondria to lysosomes via autophagosomes (Figure 8).

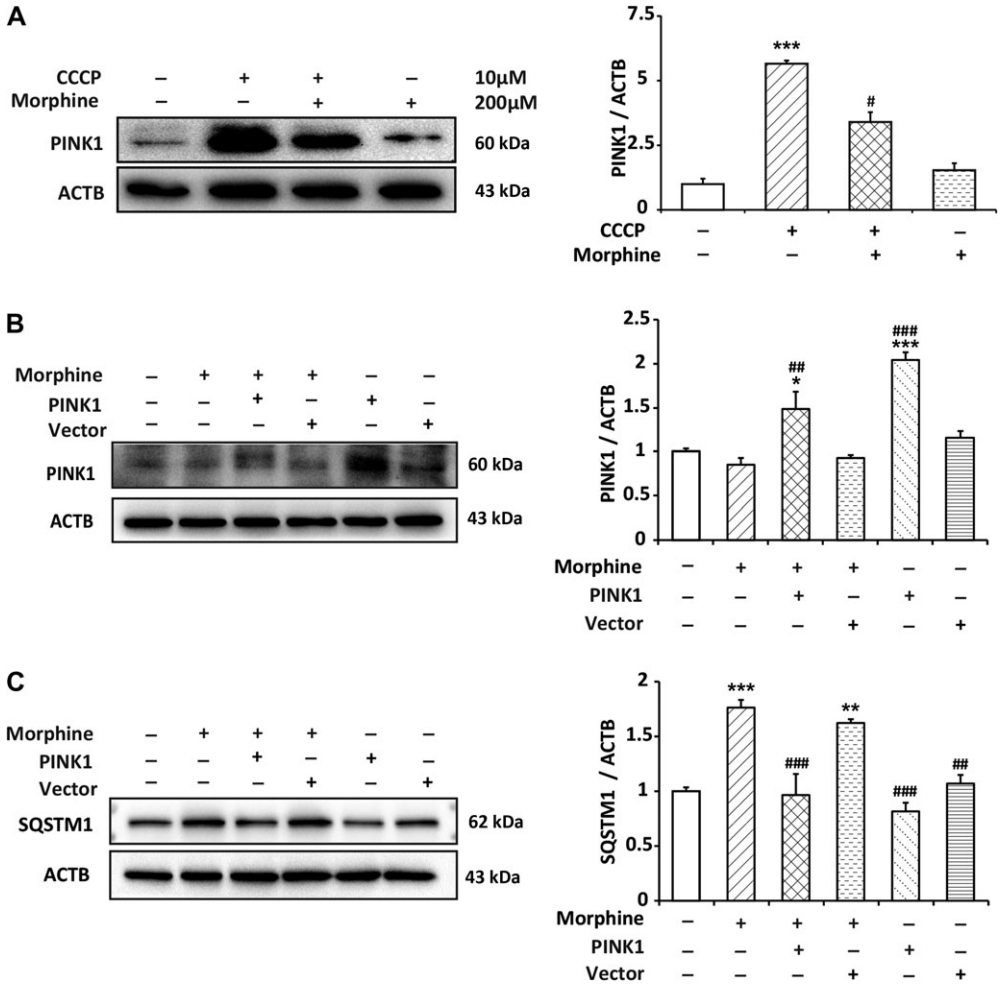

Figure 7 Morphine induces the degradation of PINK1 and the rescue of PINK1 improves the accumulation of SQSTM1/p62 induced by morphine. (**A**) SH-SY5Y cells were treated with CCCP (10 μM) for 2.5 h with or without morphine (200 μM) for 24 h. The level of PINK1 was analyzed by western blotting. $n = 3$, $^{***}P < 0.001$ vs. control group, $^{\#}P < 0.05$ vs. CCCP group. (**B** and **C**) SH-SY5Y cells were transfected with pLenti-Ubc-PINK1-2A-EGFP for 48 h, followed by morphine (200 μM) treatment for 24 h. The levels of PINK1 and SQSTM1/p62 were analyzed by western blotting. $n = 3$, $^{*}P < 0.05$, $^{**}P < 0.01$, $^{***}P < 0.001$ vs. control group, $^{\#\#}P < 0.01$, $^{\#\#\#}P < 0.001$ vs. morphine group.

For several decades, numerous scientific studies have been devoted to understanding the mechanisms of morphine tolerance including neuronal and non-neuronal actions. In this study, we illuminated that morphine administration interrupted mitophagy, a very important biological mechanism. In addition, our study manifested that morphine administration could induce mitochondria disorder. It implies that the chronic administration of opioid analgesics increases risk of dysfunction of mitochondria. Various diseases have been reported to be associated with the dysfunction of mitophagy, such as Parkinson's disease (Chu, 2011), Niemann Pick disease (Ordonez, 2012), Alzheimer's disease (Santos et al., 2010), heart failure (Chaanine et al., 2012), muscle disease (Mitsuhashi and Nishino, 2011), and cancer (Soengas, 2012). Thus, our study is also helpful for a better understanding of the dysfunction of mitophagy in diseases.

Taken together, our findings suggest a new intracellular pathway in dorsal horn neurons that underlies mechanism of morphine tolerance. Under normal conditions, this pathway is inactive. After chronic exposure, morphine inhibits mitochondria damage-induced accumulation of PINK1 and interrupts the recruitment of Parkin to the impaired mitochondria. Consequently, the ubiquitination of mitochondrial protein is inhibited, and the autophagosomes fail to recognize the damaged mitochondria. Finally, the impaired mitochondria are not delivered to lysosomes for degradation leading to robust ROS production. This reveals a novel understanding for morphine-induced mitochondrial dysfunction.

Materials and methods

Reagents and antibodies

Morphine was purchased from Shenyang First Pharmaceutical Factory, Shenyang, China. Rapamycin, 3-methyladenine (3-MA), rotenone, carbonyl cyanide 3-chlorophenylhydrazone (CCCP), and chloroquine (CQ) were purchased from Sigma. MitoSOX, MitoTracker Green FM, LysoSensor Green DND-189, LysoTracker Red DND-99, and Hoechest 33342 were from Life Technologies.

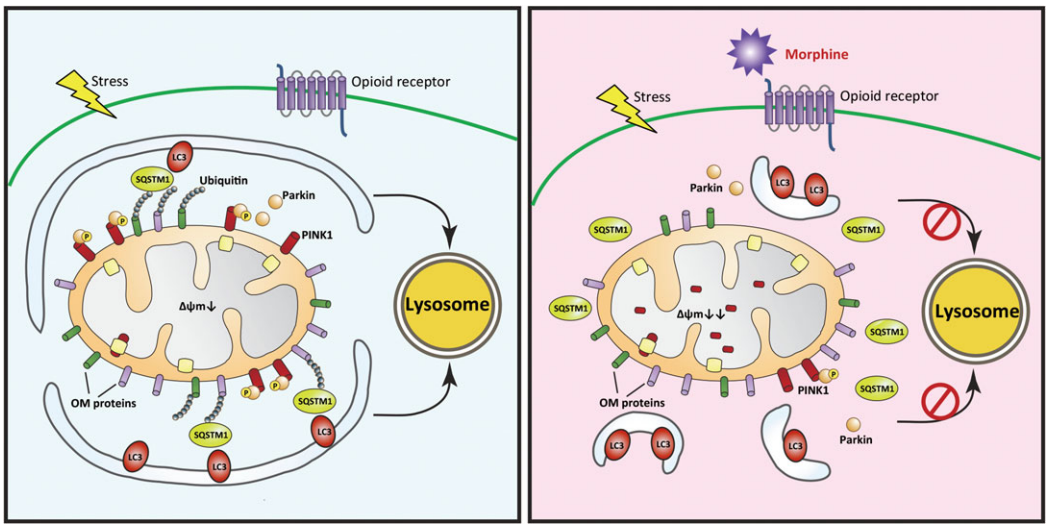

Figure 8 The schematic summary for morphine-induced suppression of mitophagy. In response to stress-induced mitochondrial damage, the $\Delta\Psi_m$ is dissipated and full-length PINK1 accumulates at the outer mitochondrial membrane (OMM). This allows for the recruitment of the ubiquitin ligase Parkin, which ubiquitinylates outer membrane proteins of mitochondria. The damaged mitochondria are rapidly recognized by autophagosomes mediated by SQSTM1/p62 and LC3. Finally, the autophagosomes containing damaged mitochondria move to lysosomes, leading to the degradation of damaged mitochondria. However, morphine inhibits the recruitment of Parkin to the damaged mitochondria and suppresses the phosphorylation of Parkin S65 by inducing the degradation of PINK1. Therefore, morphine interrupts the recognition of autophagosomes to the damaged mitochondria, and the impaired mitochondria cannot be delivered to lysosomes by autophagosomes. It leads to the accumulation of damaged mitochondria and robust production of ROS.

The primary antibodies for immunoblotting analysis were as follows: LC3A/B (CST, 4108), SQSTM1/p62 (CST, 5114), ATG-5 (CST, 12994), BECN1 (CST, 3738), BAX (CST, 2772), BCL2 (CST, 2876), Tom20 (Abcam, ab186734), COX IV (CST, 11967), PARK2 (Abcam, ab15954), PARK2-phospho S65 (Abcam, ab154995), PINK1 (CST, 6946), ATPB (Abcam, ab14730), and ACTB (CST, 4970). The secondary antibodies were from Cell Signaling Technology.

The primary antibodies for immunofluorescence analysis were as follows: SQSTM1/p62 (Abcam, ab91526/56416), NeuN (Millipore, MAB337), GFAP (Santa Cruz, sc-6170), Iba1 (Abcam, ab5076), and PARK2 (Abcam, ab15954). The secondary antibodies were from Jackson ImmunoResearch.

Animals

All procedures were strictly performed in accordance with the regulations of The Ethics Committee of the International Association for the Study of Pain and the Guide for the Care and Use of Laboratory Animals (The Ministry of Science and Technology of China, 2006). All animal experiments were approved by the Nanjing Medical University Animal Care and Use Committee and were designed to minimize suffering and the number of animals used.

Adult CD-1 mice (18–22 g wild-type) were provided by the Experimental Animal Center at Nanjing Medical University, Nanjing, China. Animals were housed 5–6 per cage under pathogen-free conditions with soft bedding under controlled temperature (22°C ± 2°C) and a 12-h light/dark cycle (lights on at 8:00 AM). Morphine was intrathecally injected at 10 μg/10 μl once a day for 7 days to establish chronic anti-nociception tolerance. Behavioral testing was performed during the light cycle (between 9:00 AM and 5:00 PM). The animals were allowed to acclimate to these conditions for at least 2 days before starting the experiments. For each group of experiments, the animals were matched by age and body weight. To assess acute analgesic effect of morphine, tail-flick test was performed every 30 min after morphine injection until 180 min. For the test of chronic tolerance, tail-flick test was performed 0.5 h after morphine administration. An equal volume of saline was given as a control. Data were calculated as percent maximal possible effect (MPE), which was calculated by the following formula: 100% × [(drug response time – basal response time) / (10 sec – basal response time)] = % MPE.

Cell lines and cell culture

Human neuroblastoma (SH-SY5Y) cells were purchased from ATCC and cultured in humidified 5% CO_2 at 37°C in Modified Eagle Media (MEM)/F12 medium supplemented with 10% (*v*/*v*) FBS, 80 U/ml penicillin, and 0.08 mg/ml streptomycin.

Western blotting

Samples (cells or spinal cord tissue segments at L1–L6) were collected and washed with ice-cold PBS before being lysed in lysis buffer. Then sample lysates were separated by SDS-PAGE and electrophoretically transferred onto polyvinylidene fluoride membranes (Millipore). The membranes were blocked with 10% whole milk in TBST (Tris-HCl, NaCl, and Tween 20) or 5% bovine serum albumin (BSA) in TBST for 2 h at room temperature, and then probed with primary antibodies at 4°C overnight. After that, bands were detected with horseradish peroxidase (HRP)-coupled

secondary antibodies. Data were acquired with the Molecular Imager (ChemiDoc, Bio-Rad) and analyzed with ImageJ software (National Institutes of Health, USA).

Quantitative PCR

Quantitative PCR was performed on SH-SY5Y cell samples and on spinal cord samples obtained from mice. Total RNA was isolated by a standard method with TRIZOL reagent (Invitrogen Life Technologies). Isolated RNA was reverse-transcribed into cDNA using PrimeScript™ RT Reagent Kit (TaKaRa) following standard protocols. Real-time quantitative PCR (qPCR) was performed with synthetic primers and SYBR Green (TaKaRa) with a QuantStudio 5 Real-Time PCR Detection System (Thermo Fisher Scientific). The relative expression level of *SQSTM1/p62* was calculated and quantified with the $2^{-\Delta\Delta Ct}$ method (Livak and Schmittgen, 2001) after normalization with the reference *GAPDH* and *ACTB* expression. All primers used are listed in Table 1.

Malondialdehyde measurement

Mice were daily intrathecally injected with saline or morphine (10 μg/10 μl) for 7 consecutive days. Spinal cord segments were collected at L1–L6. The malondialdehyde (MDA) of mouse spinal cord samples was measured according to a previously described method (Gong et al., 2012). Briefly, the tissue samples subjected to MDA measurement were assayed with kits from Nanjing Jiancheng Bioengineering Institute according to manufacturer's instructions. The products of reactions were detected by Multi-Mode Microplate Readers (Thermo Multiskan FC) at 532 nm.

ROS measurement

SH-SY5Y cells were cultured in 6-well plates and stimulated with morphine (200 μM) for 24 h. After the cultivation, supernatant was removed and cells were washed with PBS. Then the cells were incubated with MitoSOX at 2.5 μM in serum-free medium for 0.5 h at 37°C. After that, cells were washed with warm PBS, removed from plates with cold PBS containing 1% FBS, and subjected to flow cytometric analyses (Miltenyi MACSQuant Analyzer 10). The data were analyzed using FlowJo statistical software. For *in vivo* study, mice were intrathecally injected with saline or morphine (10 μg/10 μl) once a day for 7 consecutive days. Spinal cord segments samples were collected at L1–L6. The ROS level of mouse spinal cord was measured with the kit (Beyotime Institute of Biotechnology) according to the previously described method (Aranda et al., 2013). Briefly, tissues were finely minced and dissociated with trypsin enzymatic solution by incubation at 37°C for 30 min. Then the same volume of mixtures was obtained with Pasteur pipettes. The cells from the mixtures were harvested by centrifugation and washed with PBS twice. Then the samples were incubated with dichloro-dihydro-fluorescein diacetate (DCFH-DA) (40 μM) in PBS for 40 min at room temperature. After that, the samples were obtained by centrifugation, washed with PBS twice, and then lysed on ice with lysis buffer. Finally, the fluorescence (λ_{ex} = 488, λ_{em} = 525) intensity of supernatant obtained from centrifugation was measured with a multi-well spectrophotometer. The data were normalized with protein concentrations of samples.

Table 1 Sequences of primers for real-time quantitative PCR.

Gene	Sequence
Gapdh (mouse)	
Forward	5′-GGCATGGACTGTGGTCATGAG-3′
Reverse	5′-TGCACCACCAACTGCTTAGC-3′
Actin (human)	
Forward	5′-GCCAGCTCACCATGGATGAT-3′
Reverse	5′-CCTCGGCCACATTGTGAACT-3′
SQSTM1/p62 (mouse)	
Forward	5′-AGAATGTGGGGGAGAGTGTG-3′
Reverse	5′-TCTGGGGTAGTGGGTGTCAG-3′
SQSTM1/p62 (human)	
Forward	5′-CTGGGACTGAGAAGGCTCAC-3′
Reverse	5′-GCAGCTGATGGAAAGGAAAT-3′

MMP measurements

Flow cytometry was utilized to measure alterations in MMP. The cationic fluorescent dye 1,1′,3,3′-tetraethylbenzamidazolocarbocyanin iodide (JC-1; Beyotime Biotechnology) was utilized for MMP measurement (Shang et al., 2005). The staining was performed according to the manufacturer's procedures, and the MMP alterations were quantified by flow cytometry analysis (Miltenyi MACSQuant Analyzer 10). The data were analyzed using FlowJo statistical software.

Immunostaining

Under deep anesthesia, mice were perfused with saline followed by 4% paraformaldehyde in PBS. Then L4–L6 lumbar segments were dissected out and post-fixed in the same fixative. The embedded blocks were sectioned at 25 μm thickness and processed for immunofluorescence assay. Sections from each group were incubated with primary antibody overnight (NeuN, 1:300; IBA-1, 1:300; GFAP, 1:300; SQSTM1/p62, 1:100). Then the sections were washed with PBS and incubated with the secondary antibody (1:300; Jackson Laboratories) for 2 h at room temperature. After being washed for three times with PBS, the samples were investigated with Zeiss confocal microscope (LSM 710, Zeiss).

Cell imaging

SH-SY5Y cells were cultured in confocal dish. Fluorescent staining was used to detect the locations of mitochondria, lysosomes, and autophagosomes. For living cells, the imaging was directly obtained under a Zeiss confocal microscope (LSM 710, Zeiss). For fixed cells, the samples were firstly stained with fluorescent probe and then fixed with 4% paraformaldehyde for 10 min followed by primary antibody and fluorescent secondary antibody detection. Finally, the imaging was obtained with a Zeiss confocal microscope (LSM 710, Zeiss).

Evaluation of lysosomal pH changes

Changes in lysosomal pH were evaluated using the LysoSensor Green DND-189 reagents. These reagents exhibited a pH-dependent increase in fluorescence intensity upon acidification (Hurwitz et al., 1997; Zhou et al., 2012). In brief, SH-SY5Y cells were grown in confocal dish. After stimulation with morphine, the cells were incubated with 1 μM of the LysoSensor reagents for 0.5 h. Fluorescence intensity and positive staining cell were examined by flow cytometry analysis (Miltenyi MACSQuant Analyzer 10).

Transmission electron microscopy

Under deep anesthesia, mice were perfused with saline followed by 4% paraformaldehyde in PBS. Then L4–L6 lumbar segments were dissected out, pre-fixed with 5% glutaraldehyde in 0.1 M PBS, pH 7.2–7.4, and then post-fixed with 1% osmium tetroxide buffer. After dehydration in a gradient series of ethyl alcohol, tissues were embedded in epoxy resin. Ultrathin sections were stained with uranyl acetate and lead citrate, and then examined using a transmission electron microscope (JEM 1230, JOEL).

Transient transfection

SH-SY5Y cells were plated in 6-well plates and allowed to reach 40%–60% confluence at the time of transfection. mRFP-GFP-LC3 adenoviral virus purchased from HanBio Technology was used according to the manufacturer's instructions. SH-SY5Y cells were incubated in growth medium with the adenoviruses at 37°C for 2 h, and then the transfection medium was replaced with new growth medium.

For the transfection of GFP-LC3 and RFP-LC3 plasmids, SH-SY5Y cells were cultured in 6-well plates with antibiotic-free medium the day before transfection. The transfection was conducted when cells reached 40%–60% confluence using Lipofectamine 2000 (Invitrogen) and serum-free medium according to the manufacturer's instructions. After 6 h, the transfection medium was replaced with the culture medium containing 10% FBS and then incubated at 37°C in 5% CO_2.

For the transfection of PINK1, pLenti-Ubc-PINK1-2A-EGFP lentiviral virus was purchased from OBIO Technology. SH-SY5Y cells were plated in 6-well plates and the virus was used according to the manufacturer's instructions. After 24 h, the transfection medium was replaced with the culture medium containing 10% FBS and then incubated at 37°C in 5% CO_2.

Cellular fractionation and mitochondria purification

To obtain an enriched mitochondrial fraction from SH-SY5Y cells, Cell Mitochondria Isolation Kit (Beyotime Biotechnology) was utilized. Mitochondria were isolated from SH-SY5Y cells according to the manufacturer's instructions (Gong et al., 2012). Briefly, cells were homogenized with Dounce homogenizer. The nuclei and debris were removed by a 10-min centrifugation at 600× *g*, and a pellet containing mitochondria was obtained by centrifugation at 11000× *g* for 10 min. The enriched mitochondrial fraction, mitochondria-containing pellet, was finally lysed in lysis buffer with protease inhibitors and phosphatase inhibitors.

Statistical analyses

All values are expressed as mean ± SEM. Statistical analyses were performed with the Student's *t*-test for two groups or one-way ANOVA (GraphPad Software) for multiple groups. *P*-values < 0.05 were considered significant.

Supplementary material

Supplementary material is available at *Journal of Molecular Cell Biology* online.

Funding

This work was supported by grants from the National Natural Science Foundation of China (81870870 to C.-Y.J., 81202513, and 81471142), Natural Science Foundation for Young Scientists of Jiangsu Province (BK20161033), and the Key Project of Nanjing Medical University Science and Technology Innovation Foundation (2017NJMUCX004).

Conflict of interest: none declared.

References

Aranda, A., Sequedo, L., Tolosa, L., et al. (2013). Dichloro-dihydro-fluorescein diacetate (DCFH-DA) assay: a quantitative method for oxidative stress assessment of nanoparticle-treated cells. Toxicol. In Vitro *27*, 954–963.

Bailey, C.P., Llorente, J., Gabra, B.H., et al. (2009). Role of protein kinase C and mu-opioid receptor (MOPr) desensitization in tolerance to morphine in rat locus coeruleus neurons. Eur. J. Neurosci. *29*, 307–318.

Balaban, R.S., Nemoto, S., and Finkel, T. (2005). Mitochondria, oxidants, and aging. Cell *120*, 483–495.

Bekhit, M.H. (2010). Opioid-induced hyperalgesia and tolerance. Am. J. Ther. *17*, 498–510.

Bjorkoy, G., Lamark, T., Brech, A., et al. (2005). p62/SQSTM1 forms protein aggregates degraded by autophagy and has a protective effect on huntingtin-induced cell death. J. Cell Biol. *171*, 603–614.

Brookes, P.S., Yoon, Y., Robotham, J.L., et al. (2004). Calcium, ATP, and ROS: a mitochondrial love-hate triangle. Am. J. Physiol. Cell Physiol. *287*, C817–C833.

Cai, Y., Kong, H., Pan, Y.B., et al. (2016). Procyanidins alleviates morphine tolerance by inhibiting activation of NLRP3 inflammasome in microglia. J. Neuroinflammation *13*, 53.

Chaanine, A.H., Jeong, D., Liang, L., et al. (2012). JNK modulates FOXO3a for the expression of the mitochondrial death and mitophagy marker BNIP3 in pathological hypertrophy and in heart failure. Cell Death Dis. *3*, 265.

Chen, D., Gao, F., Li, B., et al. (2010). Parkin mono-ubiquitinates Bcl-2 and regulates autophagy. J. Biol. Chem. *285*, 38214–38223.

Chu, C.T. (2011). Diversity in the regulation of autophagy and mitophagy: lessons from Parkinson's disease. Parkinsons Dis. *2011*, 789431.

Ding, W.X., and Yin, X.M. (2012). Mitophagy: mechanisms, pathophysiological roles, and analysis. Biol. Chem. *393*, 547–564.

Dong, G.Z., Lee, J.H., Ki, S.H., et al. (2014). AMPK activation by isorhamnetin protects hepatocytes against oxidative stress and mitochondrial dysfunction. Eur. J. Pharmacol. *740*, 634–640.

Eiyama, A., and Okamoto, K. (2015). PINK1/Parkin-mediated mitophagy in mammalian cells. Curr. Opin. Cell Biol. *33*, 95–101.

Geisler, S., Holmstrom, K.M., Skujat, D., et al. (2010). PINK1/Parkin-mediated mitophagy is dependent on VDAC1 and p62/SQSTM1. Nat. Cell Biol. *12*, 119–131.

Goldman, S.J., Taylor, R., Zhang, Y., et al. (2010). Autophagy and the degradation of mitochondria. Mitochondrion *10*, 309–315.

Gong, K., Chen, C., Zhan, Y., et al. (2012). Autophagy-related gene 7 (ATG7) and reactive oxygen species/extracellular signal-regulated kinase regulate tetrandrine-induced autophagy in human hepatocellular carcinoma. J. Biol. Chem. *287*, 35576–35588.

Greene, A.W., Grenier, K., Aguileta, M.A., et al. (2012). Mitochondrial processing peptidase regulates PINK1 processing, import and Parkin recruitment. EMBO Rep. *13*, 378–385.

Hurwitz, S.J., Terashima, M., Mizunuma, N., et al. (1997). Vesicular anthracycline accumulation in doxorubicin-selected U-937 cells: participation of lysosomes. Blood *89*, 3745–3754.

Hutchinson, M.R., Northcutt, A.L., Hiranita, T., et al. (2012). Opioid activation of toll-like receptor 4 contributes to drug reinforcement. J. Neurosci. *32*, 11187–11200.

Hutchinson, M.R., Shavit, Y., Grace, P.M., et al. (2011). Exploring the neuroimmunopharmacology of opioids: an integrative review of mechanisms of central immune signaling and their implications for opioid analgesia. Pharmacol. Rev. *63*, 772–810.

Kane, L.A., Lazarou, M., Fogel, A.I., et al. (2014). PINK1 phosphorylates ubiquitin to activate Parkin E3 ubiquitin ligase activity. J. Cell Biol. *205*, 143–153.

Kazlauskaite, A., Kondapalli, C., Gourlay, R., et al. (2014). Parkin is activated by PINK1-dependent phosphorylation of ubiquitin at Ser65. Biochem. J. *460*, 127–139.

Keil, E., Hocker, R., Schuster, M., et al. (2013). Phosphorylation of Atg5 by the Gadd45β–MEKK4–p38 pathway inhibits autophagy. Cell Death Differ. *20*, 321–332.

Kim, P.K., Hailey, D.W., Mullen, R.T., et al. (2008). Ubiquitin signals autophagic degradation of cytosolic proteins and peroxisomes. Proc. Natl Acad. Sci. USA *105*, 20567–20574.

Kim, H.K., Park, S.K., Zhou, J.L., et al. (2004). Reactive oxygen species (ROS) play an important role in a rat model of neuropathic pain. Pain *111*, 116–124.

Kleibeuker, W., Ledeboer, A., Eijkelkamp, N., et al. (2007). A role for G protein-coupled receptor kinase 2 in mechanical allodynia. Eur. J. Neurosci. *25*, 1696–1704.

Kluck, R.M., Bossy-Wetzel, E., Green, D.R., et al. (1997). The release of cytochrome c from mitochondria: a primary site for Bcl-2 regulation of apoptosis. Science *275*, 1132–1136.

Kondapalli, C., Kazlauskaite, A., Zhang, N., et al. (2012). PINK1 is activated by mitochondrial membrane potential depolarization and stimulates Parkin E3 ligase activity by phosphorylating Serine 65. Open Biol. *2*, 120080.

Law, B.Y., Chan, W.K., Xu, S.W., et al. (2014). Natural small-molecule enhancers of autophagy induce autophagic cell death in apoptosis-defective cells. Sci. Rep. *4*, 5510.

Livak, K.J., and Schmittgen, T.D. (2001). Analysis of relative gene expression data using real-time quantitative PCR and the $2^{-\Delta\Delta Ct}$ Method. Methods *25*, 402–408.

Lu, L., Pan, C., Chen, L., et al. (2017). AMPK activation by peri-sciatic nerve administration of ozone attenuates CCI-induced neuropathic pain in rats. J. Mol. Cell Biol. *9*, 132–143.

Ma, J., Yuan, X., Qu, H., et al. (2015). The role of reactive oxygen species in morphine addiction of SH-SY5Y cells. Life Sci. *124*, 128–135.

Macey, T.A., Lowe, J.D., and Chavkin, C. (2006). Mu opioid receptor activation of ERK1/2 is GRK3 and arrestin dependent in striatal neurons. J. Biol. Chem. *281*, 34515–34524.

Martin, G., Ahmed, S.H., Blank, T., et al. (1999). Chronic morphine treatment alters NMDA receptor-mediated synaptic transmission in the nucleus accumbens. J. Neurosci. *19*, 9081–9089.

Martinou, J.C., and Green, D.R. (2001). Breaking the mitochondrial barrier. Nat. Rev. Mol. Cell Biol. *2*, 63–67.

Mitsuhashi, S., and Nishino, I. (2011). Phospholipid synthetic defect and mitophagy in muscle disease. Autophagy *7*, 1559–1561.

Miyatake, M., Rubinstein, T.J., McLennan, G.P., et al. (2009). Inhibition of EGF-induced ERK/MAP kinase-mediated astrocyte proliferation by mu opioids: integration of G protein and β-arrestin 2-dependent pathways. J. Neurochem. *110*, 662–674.

Morgan, M.M., and Christie, M.J. (2011). Analysis of opioid efficacy, tolerance, addiction and dependence from cell culture to human. Br. J. Pharmacol. *164*, 1322–1334.

Narendra, D.P., Jin, S.M., Tanaka, A., et al. (2010). PINK1 is selectively stabilized on impaired mitochondria to activate Parkin. PLoS Biol. *8*, e1000298.

Narendra, D., Tanaka, A., Suen, D.F., et al. (2008). Parkin is recruited selectively to impaired mitochondria and promotes their autophagy. J. Cell Biol. *183*, 795–803.

Nugent, F.S., Penick, E.C., and Kauer, J.A. (2007). Opioids block long-term potentiation of inhibitory synapses. Nature *446*, 1086–1090.

Ordonez, M.P. (2012). Defective mitophagy in human Niemann-Pick Type C1 neurons is due to abnormal autophagy activation. Autophagy *8*, 1157–1158.

Pankiv, S., Clausen, T.H., Lamark, T., et al. (2007). p62/SQSTM1 binds directly to Atg8/LC3 to facilitate degradation of ubiquitinated protein aggregates by autophagy. J. Biol. Chem. *282*, 24131–24145.

Renfrey, S., Downton, C., and Featherstone, J. (2003). The painful reality. Nat. Rev. Drug Discov. *2*, 175–176.

Santos, R.X., Correia, S.C., Wang, X., et al. (2010). A synergistic dysfunction of mitochondrial fission/fusion dynamics and mitophagy in Alzheimer's disease. J. Alzheimers Dis. *20 Suppl 2*, S401–S412.

Schweers, R.L., Zhang, J., Randall, M.S., et al. (2007). NIX is required for programmed mitochondrial clearance during reticulocyte maturation. Proc. Natl Acad. Sci. USA *104*, 19500–19505.

Shang, T., Joseph, J., Hillard, C.J., et al. (2005). Death-associated protein kinase as a sensor of mitochondrial membrane potential: role of lysosome in mitochondrial toxin-induced cell death. J. Biol. Chem. *280*, 34644–34653.

Soengas, M.S. (2012). Mitophagy or how to control the Jekyll and Hyde embedded in mitochondrial metabolism: implications for melanoma progression and drug resistance. Pigment Cell Melanoma Res. *25*, 721–731.

Tait, S.W., and Green, D.R. (2010). Mitochondria and cell death: outer membrane permeabilization and beyond. Nat. Rev. Mol. Cell Biol. *11*, 621–632.

Viviani, B., Bartesaghi, S., Gardoni, F., et al. (2003). Interleukin-1β enhances NMDA receptor-mediated intracellular calcium increase through activation of the Src family of kinases. J. Neurosci. *23*, 8692–8700.

Wallace, D.C., Fan, W., and Procaccio, V. (2010). Mitochondrial energetics and therapeutics. Annu. Rev. Pathol. *5*, 297–348.

Wang, X., Loram, L.C., Ramos, K., et al. (2012). Morphine activates neuroinflammation in a manner parallel to endotoxin. Proc. Natl Acad. Sci. USA *109*, 6325–6330.

Yang, J., Liu, X., Bhalla, K., et al. (1997). Prevention of apoptosis by Bcl-2: release of cytochrome c from mitochondria blocked. Science *275*, 1129–1132.

Youle, R.J., and Narendra, D.P. (2011). Mechanisms of mitophagy. Nat. Rev. Mol. Cell Biol. *12*, 9–14.

Zhou, J., Hu, S.E., Tan, S.H., et al. (2012). Andrographolide sensitizes cisplatin-induced apoptosis via suppression of autophagosome-lysosome fusion in human cancer cells. Autophagy *8*, 338–349.

Zhou, R., Yazdi, A.S., Menu, P., et al. (2011). A role for mitochondria in NLRP3 inflammasome activation. Nature *469*, 221–225.

Zong, H., Ren, J.M., Young, L.H., et al. (2002). AMP kinase is required for mitochondrial biogenesis in skeletal muscle in response to chronic energy deprivation. Proc. Natl Acad. Sci. USA *99*, 15983–15987.